Definition of roughness structures for superhydrophobic and hydrophilic optical coatings on glass

Luisa Coriand,[1,2,*] Monika Mitterhuber,[3] Angela Duparré,[1] and Andreas Tünnermann[1,2]

[1]Fraunhofer Institute for Applied Optics and Precision Engineering, Albert-Einstein-Strasse 7, 07745 Jena, Germany

[2]Friedrich-Schiller-University, Institute of Applied Physics, Max-Wien-Platz 1, 07743 Jena, Germany

[3]ETC Products GmbH, Ulrichsberger Strasse 17, 94469 Deggendorf, Germany

*Corresponding author: luisa.coriand@iof.fraunhofer.de

With specific modeling, measurement, and analysis procedures, it is possible to predict, define, and control roughness structures for tailored wetting properties of optical coatings. Examples are given for superhydrophobic and hydrophilic sol-gel layers on glass substrate.   © 2011 Optical Society of America

OCIS codes: 240.0310, 240.5770, 240.6700, 120.6660, 220.4241, 310.6870.

1. Introduction

Numerous surfaces are being cleaned with extensive use of chemicals. For glass surfaces, this concerns, e.g., windows, shower cubicles, mirrors, as well as optical components for indoor and outdoor applications. This considerable environmental impact could be significantly reduced by employing surfaces with adjustable wetting properties all the way to self-cleaning. Besides reducing the economic impact through the reduction of detergents, efficient manufacturing process strategies constitute another main key to resource conservation.

It is the roughness of a surface that, besides chemical composition, essentially governs its wetting properties [1]. Roughness structures in the micro- and nano-ranges are, hence, gaining more and more importance for implementing the desired functionalities. Superhydrophobic, hydrophilic, and anti-fog features can be achieved by a variety of stochastic, but deliberately tailored, surface roughness characteristics. This results in a promising potential for the technical fabrication of such structures, even

on the pure nanometer scale, and, hence, provides for linking the functional properties with optical quality, i.e., minimized light scattering losses [2]. Designing nanoroughness for optimal wetting properties while at the same time avoiding critical scattering losses is of crucial importance when optical superhydrophobic and hydrophilic coatings shall be achieved.

In particular, for superhydrophobic surfaces, a huge number of papers has been published (see, e.g., the comprehensive overview in [3]). To a large extent, these papers address either technology aspects of surface structuring and chemistry or theoretical studies. Furthermore, the specific aspects of optical surfaces are rarely being considered. Hence, work at the Fraunhofer Institute in Jena has been dedicated to contribute to bridging the missing links by a semiempirical approach. This approach consists of a roughness analysis procedure based on power spectral density functions, finally resulting in a universal "wetting parameter" that constitutes a reliable indicator for stochastic surface structures essentially required to create superhydrophobicity [2,4]. In this paper, we report on the measurement and analysis methodology we established on this basis for effectively predicting, defining, and controlling roughness

structures for optimal hydrophobic properties of optical surfaces. In addition, first attempts to extend the methodology to hydrophilic surfaces are described.

Examples include nanostructured hydrophobic and hydrophilic sol-gel coatings with low scatter losses on glass substrates.

2. Experimental Procedures

A. Sample Preparation

Coatings were prepared at ETC Products GmbH using a sol-gel technique and a dip-coating process [5,6]. The sol-gel coatings were deposited onto soda lime glass plates with a size of $26\,mm \times 76\,mm \times 1\,mm$.

For the hydrophobic case, Al_2O_3 films of approximately $250\,nm$ thickness were overcoated with a hydrophobic (fluoroalkylsilane) layer of about $5\,nm$ thickness using the same dip-coating technology as for the nanorough coatings. Hydrophilic coatings were realized by SiO_2 films of approximately $120\,nm$ thickness with embedded SiO_2 nanoparticles. We switched from Al_2O_3 films to SiO_2 films because SiO_2 nanoparticles were available in a larger variation of sizes and concentration. Thus, hydrophilic coatings with a large variation of roughness properties and porosity could be realized, which is important for influencing the hydrophilic wetting properties, especially the anti-fog behavior. However, the roughness nanostructures for hydrophilic, anti-fog properties could be achieved on the basis of Al_2O_3 films, as well.

B. Roughness Measurements

To analyze the wetting-relevant roughness components within the high spatial frequency range from $1\,\mu m^{-1}$ to $1000\,\mu m^{-1}$ (i.e., lateral dimension from 1000 to 1 nm) we used a Dimension 3100 atomic force microscope (AFM) from VEECO in the Tapping Mode with single crystalline silicon probes (nominal tip radius: 10 nm). For each sample, several scans were performed at different positions and in scan areas from $200\,nm \times 200\,nm$ to $10\,\mu m \times 10\,\mu m$. The image resolution amounted to 512×512 pixels, and each scan was corrected for offset and tilt. The root-mean-square roughness σ and power spectral density (PSD) functions were calculated using the program Nanoscope III from Digital Instruments.

AFM measurements can be influenced by measurement artifacts and noise. Especially at high spatial frequencies ($f > 10\,\mu m^{-1}$), the modification (distortion) of the surface profile by the nonvanishing size of the probe tip can be significant. The limits of available roughness information in this critical range were studied in a previous work [7]. The vertical resolution is limited by instrumental noise to $\sigma \approx 0.04\,nm$.

C. Wetting Measurement on Hydrophobic Surfaces

For the characterization of the hydrophobic as well as the hydrophilic wetting behavior, we used a Data-Physics OCA20 measurement system.

On real surfaces (rough and chemically heterogeneous), it is necessary to distinguish between the actual and apparent contact angles. The apparent contact angle Θ_{ap} can be measured directly and is defined as the angle between the tangent to the liquid–gas interface and the line that represents the nominal solid surface, as seen macroscopically [8].

Furthermore, wetting on rough surfaces is characterized by a wide range of metastable Θ_{ap}. For this reason, it is not sufficient to determine a static contact angle. Only on ideal surfaces (no roughness, chemically homogeneous), one single thermodynamically stable contact angle (intrinsic Young contact angle Θ_Y) exists [9].

To determine the highest and lowest values within the range of metastable contact angles of a real wetting system, the so-called advancing and receding contact angles have to be measured. Contact angles of sessile drops (initial volume of $10\,\mu l$) with varying volume (typically $50\,\mu l$) using the needle-in-drop method were measured. While increasing the drop volume, the highest observed Θ_{ap} is termed advancing contact angle Θ_{aca}. By decreasing the volume, the lowest Θ_{ap} is defined as receding contact angle Θ_{rca}. For this measurement technique, the water drop must be axially symmetric and sufficiently large compared to the scale of roughness. The difference between Θ_{aca} and Θ_{rca} is termed contact angle hysteresis [8].

The width of the contact angle hysteresis is connected to the minimum tilting angle α of the surface at which a drop starts sliding or rolling off [1,10]. Measurements of slide-off angles and roll-off angles at a defined drop volume of $35\,\mu l$ were performed by a motorized rotation of the contact angle measurement system along its horizontal axis.

On surfaces with large Θ_{aca} and large contact angle hysteresis, drops tend to stick on, rather than to slide or roll off. If a drop possesses kinetic energy, it can overcome the sticking forces [11]. We developed a testing method (bouncing test) to prove this. In doing so, a drop (volume $= 6\,\mu l$) falls on a tilted surface (tilting angle $\leq 40°$) from a height of 6 mm. The bounce-off angle α_{bo} then is defined as the minimum angle at which the drop jumps off the surface without residue.

Superhydrophobicity (see Section 3) requires high Θ_{aca} as well as low contact angle hysteresis, resulting in drops that easily roll off. Thus, understanding the contact angle hysteresis besides the contact angles is essential for understanding (super)hydrophobic wetting behavior.

D. Wetting Measurement on Hydrophilic/Anti-Fog Surfaces

For hydrophilic surfaces with $\Theta_{ap} < 20°$, Θ_{aca} and Θ_{rca} measurements fail as a result of the increased

measurement uncertainty and a vanishing Θ_{rca}. Thus, instead of the Θ_{aca} and Θ_{rca} measurements, contact angles with defined volume of $1.5\,\mu l$ were determined as a function of the wetting time t_w.

Furthermore, we established a special method to quantify the fogging behavior of hydrophilic coatings. The samples are exposed to steaming water (temperature: $50\,°C$) for $30\,s$. The condensed fog is afterward analyzed by means of microscopy and evaluated for shape and chronological development.

E. Light Scattering Measurement

Scatter losses were measured as angle resolved scattering (ARS) at a wavelength of $532\,nm$ using the instrument ALBATROSS-TT (3D-Arrangement for Laser Based Transmittance, Reflectance and Optical Scatter Measurement—Table Top), which is described in detail in [12]. Integration of the ARS yielded the total scattering (TS) losses [13].

The light scattering threshold related to optical esthetic requirements is described in detail in [14], where a reliable link between the visual inspection under different observation conditions and the measured TS levels was established. For example, the TS threshold for scattering into the transmission hemisphere was determined as $0.22\% \pm 0.03\%$.

3. Criteria of Wetting Properties

A. Superhydrophobic Surfaces

In everyday life as well as in science the term "superhydrophobic" appears very often. Nevertheless, to date there is no generally accepted definition in the literature, and alternative wording, such as ultrahydrophobic, nonwettable, extremely water repellent, superhygrophobic, etc., can be found, as well [3,15]. Even though we are aware of this varying terminology, for convenience we keep to the mostly used term superhydrophobicity. Hence, before describing the details about our methodology and the correlation between the roughness and wetting properties, the criteria used in this paper will be introduced.

In a former paper [4], we defined superhydrophobicity (which then we still called ultrahydrophobicity) by the following two theoretical criteria:

– High water contact angle $\Theta_{aca} \geq 150°$ [Fig. 1(a)] and

– low contact angle hysteresis and low roll-off angle α of $\lesssim 20°$.

To comply with both criteria, wetting has to occur necessarily in the heterogeneous wetting state [16], where air cavities are entrapped between the liquid and the solid. Essential for this wetting state is a surface with a sufficiently high aspect ratio of the roughness structure. This, in turn, is important for the self-cleaning effect based on superhydrophobicity: Because of the high aspect ratio of the roughness structure, the contact area between the particle and solid surface is considerably less than the contact area be-

tween the particle and water drop, which minimizes the adhesion forces. Thus, particles adhere to the surface of the water drops and can be removed by tilting the sample.

Regarding feasible applications of superhydrophobic surfaces, the theoretical definition of superhydrophobicity is, however, not always essential. In certain cases, a practical, less stringent consideration could be used: Surfaces with high water contact angles $\Theta_{aca} > 140°$ and low bounce-off angles $\alpha_{bo} \leq 40°$ [Fig. 1(b)] are denoted as "superhydrophobic according to practical aspects." For the sake of simplicity, we call this "highly water-repellent."

B. Hydrophilic/Anti-Fog Surfaces

Although the term "anti-fog" is often commercially used, there is a large number of different definitions. Some interesting investigations can be found in [17–19].

In our paper, hydrophilic surfaces are called anti-fog surfaces, if the apparent contact angle Θ_{ap} is less than $10°$ [Fig. 2(a)], and, thus, the condensing water wets the surface completely and instantaneously [Fig. 2(b)].

4. Methodology

Theoretical relationships between the roughness and the wetting properties were already described by Wenzel [20] and by Cassie and Baxter [21]. The application of these equations for the design of roughness structures and prediction of their wetting behavior have so far been limited to deterministic model surfaces.

For hydrophobicity, wide-scale roughness analysis by PSD functions and subsequent data reduction were found to yield a direct link between the roughness characteristics and advancing contact angle [2].

The PSD, which provides the relative strength of the individual roughness components as a function of spatial frequency f, can be calculated from surface topography data $z(x,y)$ within a certain scan range L as [22]:

$$\text{PSD}(f_x, f_y) = \lim_{L\to\infty} \frac{1}{L^2} \left| \int_0^L \int_0^L z(x,y) e^{-j2\pi(f_x x + f_y y)} \mathrm{d}x \mathrm{d}y \right|^2.$$
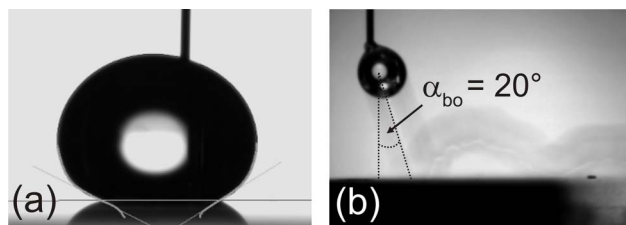
(1)

Fig. 1. (a) Superhydrophobic sol-gel coating: $\Theta_{aca} = 150°$; (b) highly water-repellent sol-gel coating: bouncing test $\alpha_{bo} = 20°$.
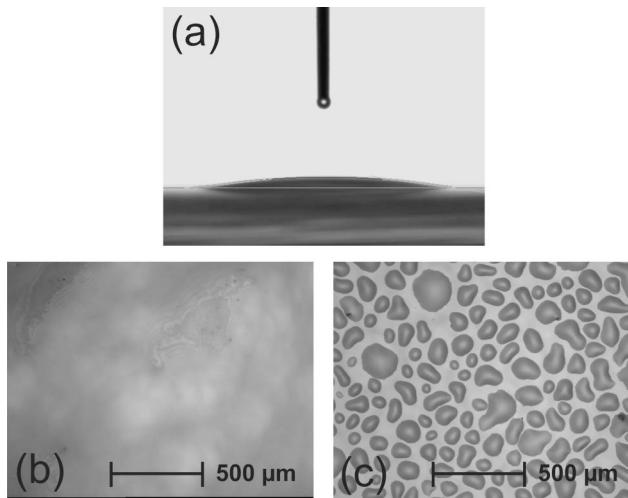
Fig. 2. (a) Hydrophilic sol-gel coating: $\Theta_{ap} = 7°$ at $t_w = 2.5\,\text{s}$; (b) hydrophilic sol-gel coating: fogging test; (c) glass substrate: fogging test.

As isotropic roughness is considered, the isotropic PSD(f) was calculated after transformation into polar coordinates and averaging over all surface directions (polar angles θ):

$$\text{PSD}(f) = \frac{1}{2\pi} \int\limits_0^{2\pi} \text{PSD}(f, \theta)\,\text{d}\theta. \qquad (2)$$

The single bandwidth-limited PSDs of a certain sample as derived from various measurements in different scan ranges were combined to a unique Master-PSD. By combining measurements performed at various scales, different surface features are captured.

Subsequent data reduction leads to a "wetting parameter" κ_B that is capable of relating the roughness characteristics to the wetting behavior of real surfaces. This means the influence of the roughness properties and the material properties on the wetting can be separated. Johnson *et al.* [23] illustrated the dependency of the wetting properties on the roughness for monoharmonic surfaces. Our approach aims at a transfer of these findings to the roughness spectrum of stochastic surfaces. In the following, a short overview of the algorithm yielding κ_B is given [4]:

1. Transformation of PSD(f) into amplitude spectrum $A(f)$,
2. reduced amplitude spectrum $A(f) \cdot f$, and
3. integration of $A(f) \cdot f$ spectrum over the logarithmic spatial frequency range.

κ_B represents a scale invariant parameter corresponding to the independence of the wetting properties of sinusoidal surface structures of their absolute magnitudes.

Our earlier experimental investigations revealed κ_B as empirically related to the water contact angle and, hence, to the wetting behavior. Using this relation between the roughness and wetting properties, κ_B of at least 0.4 was found to be necessary for potential superhydrophobicity [4]. It is very important to note that this criterion constitutes an *essential* condition, *not a sufficient* one.

Utilizing the κ_B approach can support the entire chain of a technological process for the fabrication of nanostructured superhydrophobic surfaces (Fig. 3) in a twofold way: First, it defines the appropriate roughness in the design process in contrast to conventional trial and error approaches. Second, it enables the separate control and characterization of the wetting effect of the fabricated roughness structures independently of the hydrophobic material properties.

As to hydrophilic properties, we are still at the beginning of studies regarding a correlation between κ_B and roughness-induced superhydrophilicity. From theory, we expect that the method should work in a similar way for the hydrophilic as for the hydrophobic domain. For this purpose, experimental analysis according to the process chain shown in Fig. 3 is required. First results are presented in Subsection 5.B.
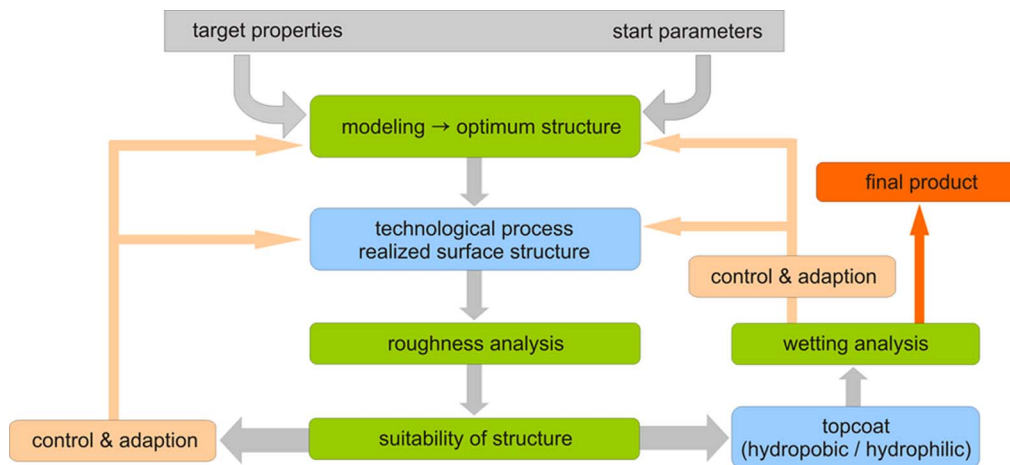

Fig. 3. (Color online) Process chain for superhydrophobic surfaces.

5. Results and Discussion

A. Hydrophobic, Highly Water-Repellent, and Superhydrophobic Al_2O_3 Coatings with Low Scattering Losses

The nanostructures of the hydrophobic and superhydrophobic sol-gel coatings are presented in Fig. 4, with the subsequent roughness analysis by PSD functions compared with the results for bare glass depicted in Fig. 5. The AFM images and PSD functions represent three different samples with κ_B values of 0.1 (sample #1), 0.3 (sample #2), and 0.7 (sample #3). κ_B of sample #3 clearly exceeds the threshold and, hence, the potential for superhydrophobicity was stated.

Results of the wetting analysis for the hydrophobic Al_2O_3 coatings are given in Fig. 6. For sample #3, the prediction of superhydrophobicity was confirmed by the measured high advancing and receding contact angles of $\Theta_{aca} = 156°$ and $\Theta_{rca} = 129°$ (i.e., contact angle hysteresis as low as 30°), as well as the small roll-off angle of $\alpha = 13°$. The self-cleaning effect of this sample, resulting from the superhydrophobicity, is demonstrated in Fig. 7: A spherical water drop rolls off the surface and removes artificial contaminants (graphite powder) on its track.

For sample #2, a promising advancing contact angle of 148° was obtained, but water drops on the tilted ($\alpha = 48°$) surface slid off owing to the rather high contact angle hysteresis of 62°. Hence, according to the definition in Subsection 3.A, sample #2 is

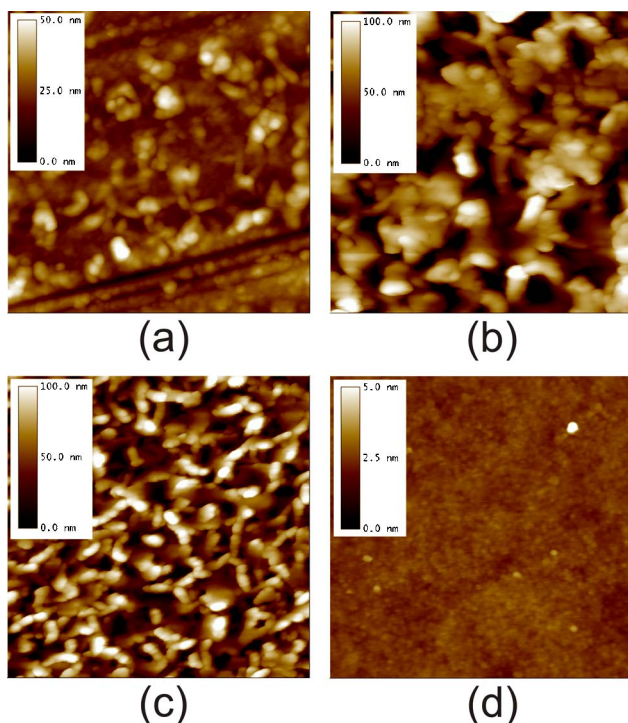Fig. 4. (Color online) AFM images (field of view $1\,\mu m \times 1\,\mu m$): Al_2O_3 sol-gel coatings [(a) sample #1, $\sigma = 6.5\,nm$; (b) sample #2, $\sigma = 24\,nm$; (c) sample #3, $\sigma = 24\,nm$] and (d) bare glass substrate ($\sigma = 0.2\,nm$).
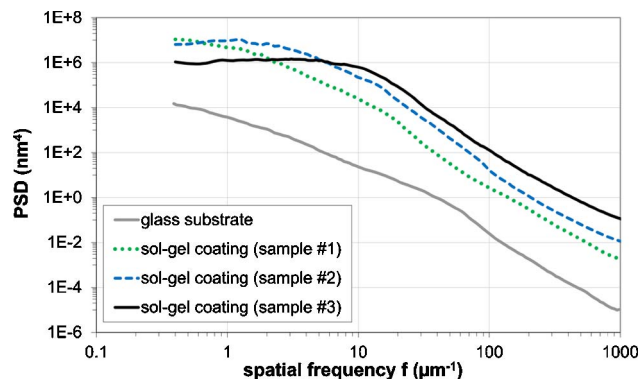

Fig. 5. (Color online) PSD functions of bare glass substrate and Al_2O_3 sol-gel coatings.

termed as highly water-repellent, because of the low bounce-off angle ($\alpha_{bo} = 20°$) visible in Fig. 8(b).

The sample with the lowest κ_B value of 0.1 exhibits quite small contact angles ($\Theta_{aca} = 124°$ and $\Theta_{rca} = 70°$), and the bouncing test in Fig. 8(a) reveals falling water drops sticking on the tilted (40°) surface.

The results of light scattering measurements at a wavelength of 532 nm are shown in Fig. 9. Even though the scattering was highest for the superhydrophobic sample #3, its overall scatter loss was as low as $TS = 0.08\%$ (transmission direction) and, hence, remained well below the threshold determined by optically esthetic requirements. Thus, the combination of enhanced nanoroughness for superhydrophobicity with low, tolerable scattering losses was successful, because the main parts of the higher roughness needed for the wetting property occur in the high spatial frequency range where roughness contributions are not decisive for scattering losses in the visible region.

B. Hydrophilic SiO_2 Coatings

The roughness analysis based on AFM measurements and PSD functions (Fig. 10) of SiO_2 coatings results in κ_B values of 0.1 (sample #4) and 0.6 (sample #5). For sample #5, we expect distinct hydrophilicity according to the theoretical assumption that increased roughness results in an enhancement of the wetting behavior.
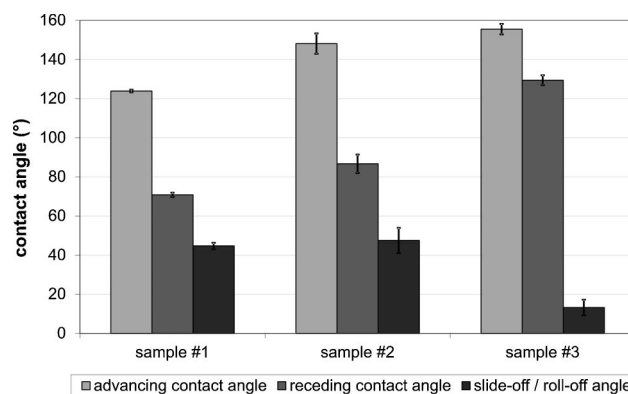

Fig. 6. Contact angles and slide-off/roll-off angles of Al_2O_3 sol-gel coatings.
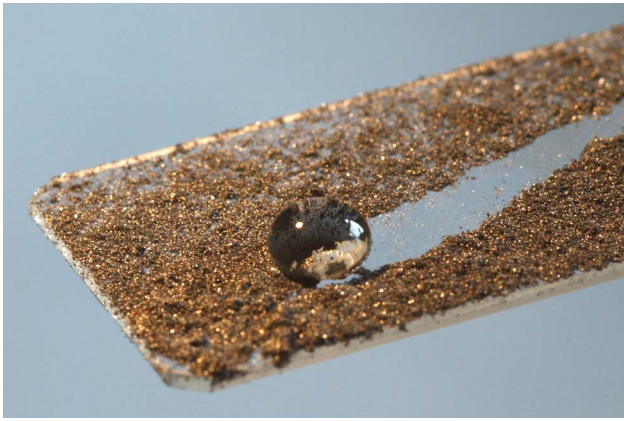
Fig. 7. (Color online) Self-cleaning effect on a glass surface with superhydrophobic coating (sample #3).

Fig. 9. (Color online) ARS measurements of bare glass substrate and Al_2O_3 sol-gel coatings.

Experimentally for sample #5, apparent contact angles of $\Theta_{ap} = 12°$ (wetting time $t_w = 0\,s$) and $< 3°(0\,s < t_w < 3\,s)$ were observed. Furthermore, the fogging test exhibits that condensing water wets the hydrophilic surface completely and instantaneously. Hence, the SiO_2 coating reveals the anti-fog effect as demonstrated in Fig. 11. In contrast, the hydrophilic behavior of sample #4 is less pronounced due to its lower surface roughness: $\Theta_{ap} = 22°(t_w = 0\,s)$, $\Theta_{ap} = 7°(0\,s < t_w < 3\,s)$, and condensing water wets the surface only partly.

From ARS measurements, TS values (transmission direction) of 0.28% (sample #4) and 4.02% (sample #5) were determined. The considerable difference of the scatter losses between the two samples probably results not only from the enhanced roughness, but also from increased porosity.

6. Conclusion and Future Challenges

A methodology based on a wetting parameter κ_B has been demonstrated to predict, define, and control roughness structures for optimal hydrophobic wetting behavior. κ_B is calculated by a specific roughness analysis, which includes PSD functions determined from AFM topography data and subsequent data reduction. To control the predictions of the wetting behavior, advancing and receding contact angle, as well as slide-off/roll-off angle measurements, were performed. A bouncing test was established to be used as a practical, less stringent criterion of superhydrophobicity.

For Al_2O_3 sol-gel coatings with graded stochastic nanostructures, we predicted the potential of the
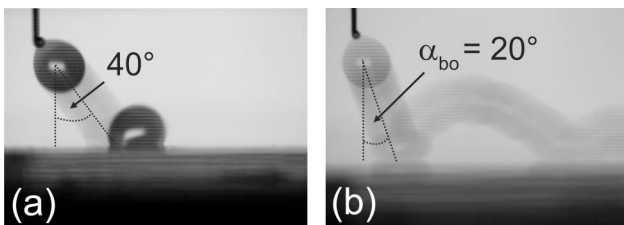
structures to generate superhydrophobicity. Afterward, the prediction was verified by wetting analysis. Furthermore, the pure nanostructure made it possible to reconcile the basically contradictory effects of necessary roughness (regarding superhydrophobicity) and undesired roughness (regarding light scattering). Nanorough Al_2O_3 sol-gel coatings (with thin hydrophobic film on top) exhibited superhydrophobicity with an advancing contact angle of 156°, low hysteresis of 30°, and a roll-off angle of 13°.

The presented methodology can be applied not only to Al_2O_3 sol-gel coatings, but also to other materials and coating processes, such as magnetron sputtered oxide films [4]. Future investigations will attempt to derive a sufficient criterion for the prediction of potential superhydrophobicity. For this purpose, the phase information of the roughness characteristic shall be considered.

Furthermore, first results were presented for hydrophilic surfaces aiming at anti-fog behavior. This wetting behavior was realized by SiO_2 sol-gel coatings and characterized by apparent contact angle measurements, as well as by fogging tests. The new fogging test was introduced to quantify the anti-fogging behavior of hydrophilic coatings. The rough-
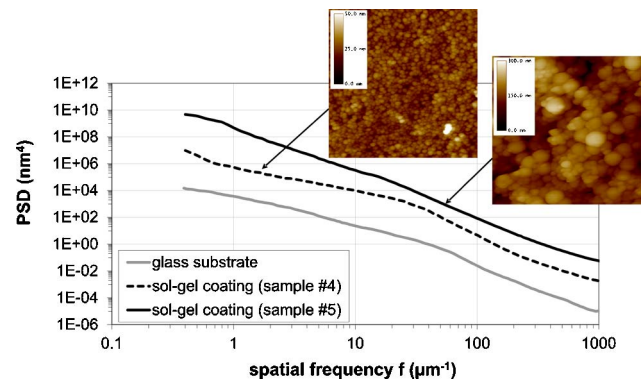

Fig. 8. Bouncing test of Al_2O_3 sol-gel coatings: (a) sample #1; (b) sample #2.

Fig. 10. (Color online) PSD functions of bare glass substrate and hydrophilic SiO_2 sol-gel coatings including AFM topography images (field of view: $1\,\mu m \times 1\,\mu m$) of hydrophilic SiO_2 sol-gel coatings (sample #4, $\sigma = 4.3\,nm$; sample #5, $\sigma = 38\,nm$).

Fig. 11. (Color online) Fogging test: bank note viewed through a glass plate with (half-side) hydrophilic coating (left, uncoated; right, coated).

ness analysis procedure using PSD functions and κ_B values was applied to these samples, as well.

Further extension of the κ_B method to hydrophilic surfaces and, hence, correlation of roughness and hydrophilic wetting properties will be pursued in future work.

References

1. E. Wolfram, R. Faust, and Wetting, *Spreading and Adhesion*, J. F. Padday, ed. (Academic, 1987), pp. 213–222.
2. M. Flemming and A. Duparré, "Design and characterization of nanostructured ultrahydrophobic coatings," Appl. Opt. **45**, 1397–1401 (2006).
3. P. Roach, N. J. Shirtcliffe, and M. I. Newton, "Progess in superhydrophobic surface development," Soft Matter **4**, 224–240 (2008).
4. M. Flemming, L. Coriand, and A. Duparré, "Ultra-hydrophobicity through stochastic surface roughness," J. Adhes. Sci. Technol. **23**, 381–400 (2009).
5. J. C. Brinker and A. J. Hurd, "Fundamentals of sol-gel dipcoating," J. Phys. III **4**, 1231–1242 (1994).
6. K. Tadanaga, N. Katata, and T. Minami, "Formation process of super-water-repellent Al_2O_3 coating films with high transparency by the sol-gel method," J. Am. Ceram. Soc. **80**, 3213–3216 (2005).
7. M. Flemming, K. Roder, and A. Duparré, "Scanning force microscopy for optical surface metrology," Proc. SPIE **5965**, 59650A (1997).
8. A. Marmur, "Soft contact: measurement and interpretation of contact angles," Soft Matter **2**, 12–17 (2006).
9. A. Marmur, "Equilibrium contact angles: theory and measurement," Colloids Surf. A **116**, 55–61 (1996).
10. E. Bittoun and A. Marmur, "Optimizing super-hydrophobic surfaces: criteria for comparison of surface topographies," J. Adhes. Sci. Technol. **23**, 401–411 (2009).
11. D. Bartolo, F. Bouamrirene, E. Verneuil, A. Buguin, P. Silberzan, and S. Moulinet, "Bouncing or sticky droplets: impalement transitions on superhydrophobic micropatterned surfaces," Europhys. Lett. **74**, 299–305 (2006).
12. A. von Finck, M. Hauptvogel, and A. Duparré, "Instrument for close-to-process light scatter measurements of thin film coatings and substrates," Appl. Opt. **50**, to appear in the same feature issue.
13. J. Stover, *Optical Scattering: Measurement and Analysis*, 2nd ed., Press Monograph Vol. PM24SC (SPIE, 1995).
14. M. Flemming, K. Reihs, and A. Duparré, "Characterization procedures for nanorough ultra-hydrophobic surfaces with controlled optical scatter," Proc. SPIE **5188**, 146–253 (2003).
15. A. Marmur, "From hygrophilic to superhygrophobic: theoretical conditions for making high-contact-angle surfaces from low-contact-angle materials," Langmuir **24**, 7573–7579 (2008).
16. A. Marmur, "The lotus effect: superhydrophobicity and metastability," Langmuir **20**, 3517–3519 (2004).
17. F. C. Cebeci, Z. Wu, L. Zhai, R. E. Cohen, and M. F. Rubner, "Nanoporosity-driven superhydrophilicity: a means to create multifunctional antifogging coatings," Langmuir **22**, 2856–2862 (2006).
18. W. S. Law, S. W. Lam, W. Y. Gan, J. Scott, and R. Amal, "Effect of film thickness and agglomerate size on the superwetting and fog-free characteristics of TiO_2 films," Thin Solid Films **517**, 5425–5430 (2009).
19. W. Y. Gan, S. W. Lam, and K. Chiang, "Novel TiO_2 thin film with non-UV activated superwetting and antifogging behaviours," J. Mater. Chem. **17**, 952–954 (2007).
20. R. N. Wenzel, "Resistance of solid surfaces to wetting by water," Ind. Eng. Chem. **28**, 988–944 (1936).
21. A. B. D. Cassie and S. Baxter, "Wettability of porous surfaces," Trans. Faraday Soc. **40**, 546–551 (1944).
22. A. Duparré, J. Ferre-Borrull, S. Gliech, G. Notni, J. Steinert, and J. M. Bennett, "Surface characterization techniques for determining the root-mean-square roughness and power spectral densities of optical components," Appl. Opt. **41**, 154–171 (2002).
23. R. E. Johnson, R. H. Dettre, and R. F. Gould, "1. Study of an idealized rough surface," in *Contact Angle, Wettability and Adhesion* (American Chemical Society, 1964), pp. 112–135.
24. R. H. DettreR. E. Johnson, and R. F. Gould, "2. Contact angles measurements on rough surfaces," in *Contact Angle, Wettability and Adhesion* (American Chemical Society, 1964), pp. 136–144.